JOURNAL OF VIROLOGY, Jan. 2011, p. 32–42 Vol. 85, No. 1
0022-538X/11/$12.00 doi:10.1128/JVI.01673-10

Function of the Small Hydrophobic Protein of J Paramyxovirus▽

Zhuo Li,[1] Jie Xu,[2] Jui Patel,[2] Sandra Fuentes,[1,2] Yuan Lin,[1] Danielle Anderson,[3]# Kaori Sakamoto,[4] Lin-Fa Wang,[3] and Biao He[1]*

Department of Infectious Disease, College of Veterinary Medicine, University of Georgia, Athens, Georgia 30602[1]; Department of Veterinary and Biomedical Sciences, Pennsylvania State University, University Park, Pennsylvania 16802[2]; CSIRO Livestock Industries, Australian Animal Health Laboratory, Private Bag 24 Geelong, Victoria 3220, Australia[3]; and Department of Pathology, College of Veterinary Medicine, University of Georgia, Athens, Georgia 30602[4]

Received 9 August 2010/Accepted 20 October 2010

At 18,954 nucleotides, the J paramyxovirus (JPV) genome is one of the largest in the family *Paramyxoviridae*, consisting of eight genes in the order 3′-N-P/V/C-M-F-SH-TM-G-L-5′. To study the function of novel paramyxovirus genes in JPV, a plasmid containing a full-length cDNA clone of the genome of JPV was constructed. In this study, the function of the small hydrophobic (SH) protein of JPV was examined by generating a recombinant JPV lacking the coding sequence of the SH protein (rJPVΔSH). rJPVΔSH was viable and had no growth defect in tissue culture cells. However, more tumor necrosis factor alpha (TNF-α) was produced during rJPVΔSH infection, suggesting that SH plays a role in inhibiting TNF-α production. rJPVΔSH induced more apoptosis in tissue culture cells than rJPV. Virus-induced apoptosis was inhibited by neutralizing antibody against TNF-α, suggesting that TNF-α contributes to JPV-induced apoptosis *in vitro*. The expression of JPV SH protein inhibited TNF-α-induced NF-κB activation in a reporter gene assay, suggesting that JPV SH protein can inhibit TNF-α signaling *in vitro*. Furthermore, infection of mice with rJPVΔSH induced more TNF-α expression, indicating that SH plays a role in blocking TNF-α expression *in vivo*.

The family *Paramyxoviridae* is classified into two subfamilies: the *Paramyxovirinae* and the *Pneumovirinae* (21). The subfamily *Paramyxovirinae* contains five genera: *Avulavirus*, *Henipavirus*, *Morbillivirus*, *Respirovirus*, and *Rubulavirus*, as well as a group of unclassified paramyxoviruses which includes J paramyxovirus (JPV), Beilong virus (BeiPV), Fer-de-lance virus, Menangle virus, Mossman virus, Salem virus, and Tupaia paramyxovirus. JPV was isolated from moribund mice (*Mus musculus*) trapped in Northern Queensland, Australia, in 1972 (19). It was reported that the four mice from which the virus was isolated had extensive hemorrhagic lung lesions. Syncytial formation was observed in kidney autoculture monolayers, and electron microscopy revealed virion morphology and nucleocapsid structure typical of the paramyxoviruses. The full-length genome of JPV has been sequenced and contains 18,954 nucleotides (17). The genome organization of JPV is 3′-N-P/V/C-M-F-SH-TM-G-L-5′. The G gene is the largest among all paramyxovirus attachment protein genes sequenced to date. The G gene encodes a putative 709-amino-acid (aa)-residue attachment protein and distally contains a second open reading frame (termed ORF-X) which is 2,115 nucleotides long. Probes specific to the G protein coding region and ORF-X both identified an mRNA species corresponding to the predicted length of the G gene. JPV contains a small hydrophobic (SH) protein gene, which is not present in all paramyxoviruses, and a unique TM gene. Northern blot analyses indicated that the putative transcription initiation and termination sequences flanking the SH and TM genes were functional, consistent with their allocation as discrete genes (16). While the SH and TM proteins were both detected in infected cells, no evidence has yet been found for the expression of ORF-X. The novel TM protein is a type II glycosylated integral membrane protein, orientated with its C terminus exposed at the cell surface.

SH protein is expressed in some but not all paramyxovirus-infected cells (21). Rubulaviruses, parainfluenza virus 5 (PIV5), formerly known as simian virus 5 (SV5) (4), and mumps virus (MuV) contain the SH gene (7, 14). The PIV5 SH gene is located between the F and HN genes. PIV5 SH protein is a type II membrane protein, containing 44 aa residues with a predicted C-terminal ectodomain of 5 residues, a transmembrane domain of 23 residues, and an N-terminal cytoplasmic tail of 16 residues (15). PIV5 SH was not essential for virus growth in tissue culture cells, and the recombinant virus lacking the SH gene (rPIV5ΔSH) could grow as well as wild-type PIV5 (10). However, rPIV5ΔSH caused increased cytopathic effect (CPE) and induced apoptosis in MDBK cells and L929 cells through the tumor necrosis factor alpha (TNF-α)-mediated extrinsic apoptotic pathway (11, 23). MuV SH protein is a type I membrane protein of 57 residues. The SH gene has been identified in all strains of MuV; however, the expression of the SH gene does not appear to be required for virus growth *in vitro* (27, 28). Although there is no sequence homology between PIV5 SH and MuV SH protein, MuV SH had a function similar to that of PIV5 SH when the ORF of PIV5 SH was replaced

* Corresponding author. Mailing address: Department of Infectious Diseases, College of Veterinary Medicine, University of Georgia, 501 D. W. Brooks Drive, Athens, GA 30602. Phone: (706) 542-2855. Fax: (706) 542-5771. E-mail: bhe@uga.edu.

Present address: INRS-Institut Armand-Frappier, Université du Québec, Laval, Québec H7V 1B7, Canada.

▽ Published ahead of print on 27 October 2010.

with the ORF of MuV SH (31). Respiratory syncytial virus (RSV), a member of subfamily *Pneumovirinae*, also encodes an SH protein (5, 6). RSV lacking the SH gene was viable, caused syncytium formation, and grew as well as wild-type virus (3, 9, 18, 20). RSVΔSH infection caused significantly more apoptosis in L929 and A549 cells (9). RSVΔSH virus resembled the wild-type recombinant virus in its efficiency of replication in the lower respiratory tract, whereas it replicated 10-fold less efficiently in the upper respiratory tract (18, 20).

The JPV SH gene is located immediately downstream from the F gene, a position analogous to that of the SH gene of rubulaviruses (16, 17). The JPV SH protein is similar to that of other paramyxoviruses in size and is a type I membrane protein, containing 69 aa residues with a predicted N-terminal ectodomain of 5 residues, a transmembrane domain of 23 residues, and a C-terminal cytoplasmic tail of 41 residues (17). In this work, we hypothesized that the JPV SH protein is a functional counterpart of the SH proteins of PIV5, MuV, and RSV. To test this, we have generated a reverse genetics system for JPV and obtained a recombinant JPV lacking SH (rJPVΔSH). We have analyzed rJPVΔSH in comparison to rJPV *in vitro* and *in vivo*.

MATERIALS AND METHODS

Cells. Monolayer cultures of BSR-T7 cells (2) were maintained in Dulbecco's modified Eagle's medium (DMEM) containing 10% fetal bovine serum (FBS), 10% tryptose phosphate broth (TPB), and 400 μg/ml G418. Monolayer cultures of Vero cells and L929 cells were maintained in DMEM containing 10% FBS, 100 IU/ml penicillin, and 100 μg/ml streptomycin. All cells were incubated at 37°C, 5% CO_2. Virus-infected cells were grown in DMEM containing 2% FBS. Plaque assays were performed on Vero cells.

Construction of recombinant viruses. A complete cDNA of the 18,954-nucleotide JPV genome was constructed from plasmids carrying the genes for N, P, M, F, SH, TM, G, and L. PCRs were applied to provide adaptor DNAs over some of the intercistronic junction, leader, and trailer sequences using a backbone plasmid from a parainfluenza virus 5 infectious cDNA clone (13). Plasmids were constructed using standard molecular biology techniques. A NotI sequence tag was introduced in the 3′ noncoding region of ORF-X. The construct containing the complete JPV genome was designated pJPV. An enhanced green fluorescent protein (EGFP) gene was inserted between the F and the SH genes. To transcribe the extra gene, gene end (GE) and gene start (GS) sequences were inserted into the 5′ noncoding region of the SH gene after the ORF of the EGFP gene. The proposed F-SH end/start sequences [TAAATAAAAA (intercistronic 3 nucleotides CTT) AGGACAAAAG] were used. The construct containing EGFP was designated pJPV-EGFP. The ORF of the SH gene was replaced with the *Renilla* luciferase (Rluc) gene. The construct lacking the SH gene and containing the Rluc gene was designated pJPVΔSH.

The plasmids, pJPV carrying the full-length genome of JPV, pJPV-EGFP carrying the full-length genome of JPV with the EGFP gene insertion, or pJPVΔSH carrying the full-length genome of JPV but with the SH gene replaced with the extra Rluc gene, and three helper plasmids pJPV-N, pJPV-P, and pJPV-L carrying genes for the N, P, and L proteins, were cotransfected into BSR-T7 cells at 95% confluence in 6-cm plates with Plus and Lipofectamine (Invitrogen). The amounts of plasmids used were as follows: 5 μg pJPV/pJPV-EGFP/pJPVΔSH, 1 μg pJPV-N, 0.3 μg pJPV-P, and 1.5 μg pJPV-L. After 3 h of incubation, the transfection medium was replaced with DMEM containing 10% FBS and 10% TPB. After 72 h of incubation at 37°C, 1/10 of the BSR-T7 cells were passed into a T-75 (75 cm^2) flask containing 1×10^6 Vero cells. The mixed cells were cocultured for 2 weeks with passaging at 3- or 4-day intervals. The medium was harvested, and cell debris was pelleted by low-speed centrifugation (3,000 rpm for 10 min). Plaque assays were used to purify single clones of the recombinant viruses. Recombinant viruses recovered from cDNA were designated rJPV, rJPV-EGFP, or rJPVΔSH.

RT-PCR and nucleotide sequencing. Total RNAs from rJPV-, rJPV-EGFP-, or rJPVΔSH-infected Vero cells were purified using an RNeasy kit (Qiagen, Inc., Valencia, CA). cDNAs were prepared using random hexamers, and aliquots of the cDNA were then amplified in reverse transcription (RT)-PCRs using appropriate oligonucleotide primer pairs. Primers p70 (GCCAA TTAGTCCCTGCGATT) and p71 (ACACGGGTTCTTGCACAACT) were used to identify rJPV. Primers p80 (CTGGGACGAGAACGGTCTTA) and p146 (CAGCTTGCCTGTGACTATGG) were used to identify the NotI sequence tag of rJPV. Primers p61 (CAACGAGTCGATCAACAAGTCTC ATG) and p94 (CATCTTCTAGGTAATGCTGGTAACCC) were used to identify rJPVΔSH. The improved rapid amplification of cDNA ends (RACE) PCR was used to amplify the leader and trailer sequences. The sequences of all primers for sequencing of the complete genomes of rJPV, rJPV-EGFP, and rJPVΔSH are available on request. DNA sequences were determined using an Applied Biosystems sequencer (ABI, Foster City, CA).

Fluorescence microscopy. To confirm the rescued rJPV, Vero cells were mock infected with or infected with rJPV. At 2 days postinfection (d.p.i.), the cells were washed with phosphate-buffered saline (PBS) and then were fixed in 0.5% formaldehyde. The cells were permeabilized in 0.1% PBS–saponin solution and incubated for 30 min with polyclonal anti-TM rabbit serum at a 1:100 dilution (Genscript USA, Inc., Piscataway, NJ), and then fluorescein isothiocyanate (FITC)-labeled goat anti-rabbit antibody was added to the cells. The cells were incubated for 30 min and were examined and photographed using a Nikon FXA fluorescence microscope.

To confirm the rescue of rJPV-EGFP, Vero cells were infected with rJPV or rJPV-EGFP. At 2 d.p.i., the cells were photographed using a Nikon FXA fluorescence microscope.

To confirm the rescue of rJPVΔSH, Vero cells were mock infected or infected with rJPV or rJPVΔSH. At 2 d.p.i., the cells were treated as described above. The permeabilized cells were incubated with polyclonal anti-TM or SH rabbit serum and then examined and photographed using a Nikon FXA fluorescence microscope.

The p65 subunit of NF-κB was examined as described previously (23). Briefly, L929 cells were mock infected or infected with rJPV or rJPVΔSH. At 1 d.p.i., cells were processed as described above. The cells were incubated with rabbit monoclonal antibody specific for the p65 subunit of the NF-κB transcription factor (Santa Cruz Biotechnology, Santa Cruz, CA). The cells were examined and photographed using a Nikon FXA fluorescence microscope.

Growth kinetics. Vero cells in 12-well plates were infected with rJPV or rJPVΔSH at an MOI of 5 or 0.1. The cells were then washed with PBS and maintained in DMEM–2% FBS. The medium was collected at 0, 24, 48, 72, and 96 hours postinfection (h p.i.). The titers of viruses were determined by plaque assay on Vero cells.

Immunoprecipitation of polypeptides. Vero cells were mock infected or infected with rJPV or rJPVΔSH. At 22 h p.i., the cells were labeled for 2 h with ^{35}S-Met/Cys Promix (100 μCi/ml). The cells were lysed in radioimmunoprecipitation buffer, and aliquots immunoprecipitated using polyclonal anti-P C-terminal or anti-V C-terminal rabbit serum (Genscript USA, Inc., Piscataway, NJ). The precipitated proteins were resolved by 15% SDS–PAGE, and then the proteins were examined by autoradiography using a Storm phosphorimager (Molecular Dynamics, Inc., Sunnyvale, CA).

Luciferase assay. The rJPVΔSH genome contains the *Renilla* luciferase gene in the place of the SH gene. To examine Rluc expression in virus-infected cells, 24 wells of Vero cells were mock infected or infected with rJPV or rJPVΔSH. At 1 d.p.i., the cells were washed and lysed with 100 μl of 1× passive lysis buffer. Ten microliters of lysate from each well were used to examine the *Renilla* luciferase activity with a luciferase assay system (Promega Corporation, Madison WI).

To examine whether JPV SH protein can inhibit TNF-α-induced NF-κB activation, 24 wells of L929 cells were transfected with an empty pCAGGS vector, pCAGGS-PIV5 SH, or pCAGGS-JPV SH plus pκB-TATA-Luc and pRL-TK. The cells were incubated at 37°C with 5% CO_2 for 18 to 24 h, and then the medium was replaced with either 250 μl of Opti-MEM alone or 250 μl of Opti-MEM containing 10 ng/ml TNF-α (catalog no. 522-009; Alexis, San Diego, CA) or 250 μl of Opti-MEM containing 50 ng/ml of the phorbol ester phorbol 12-myristate 13-acetate (PMA) (catalog no. p1585; Sigma, St. Louis, MO), and cells were incubated for 4 h at 37°C with 5% CO_2. The luciferase activity, expressed as the ratio of firefly luciferase activity to *Renilla* luciferase activity, was measured using a Veritas microplate luminometer (Turner Biosystems) to indicate the expression levels of the reporter gene under the control of the NF-κB element. The fold increase and the ratio of the amount

of luciferase activity of TNF-α-treated cells to that of untreated cells were used to indicate the effect of SH on TNF-α signaling.

UV inactivation of viruses. L929 cells were mock infected or infected with rJPV or rJPVΔSH at an MOI of 5. At 2 d.p.i., the plate was uncovered, placed inside a Fisher Hamilton biological safety cabinet class II, and UV treated for 30 min. The medium was then filtered through a 0.22-μm filter to remove cell debris. The effectiveness of the UV treatment in inactivating JPV was confirmed by plaque assay.

Enzyme-linked immunosorbent assay (ELISA) of TNF-α. L929 cells were mock infected or infected with rJPV or rJPVΔSH at an MOI of 5. The medium was collected at different time points postinfection. The amounts of TNF-α were measured by using a murine TNF-α detection kit purchased from Amersham Pharmacia (Piscataway, NJ) according to the manufacturer's instructions. Amounts of 50 μl of medium from infected cells or standards in duplicate and 50 μl of biotinylated antibody against TNF-α were added to strips prelabeled with antibody against TNF-α. The strips were incubated at room temperature for 2 h. After the strips were washed three times with wash buffer provided by the manufacturer, 100 μl of streptavidin-horseradish peroxidase conjugate was added, and they were incubated at room temperature for 30 min. The strips were then washed three times, and 100 μl of 3,3′,5,5′-tetramethylbenzidine substrate solution was added to each well. The strips were incubated in the dark at room temperature for 30 min, and 100 μl of stop solution was added to each well. The optical density at 450 nm was measured within 30 min. The amounts of TNF-α were calculated by using standard curves generated from known concentrations of TNF-α provided by the manufacturer.

Apoptosis assay. Fragmented DNAs were purified as described previously. Briefly, confluent L929 cells were mock infected or infected with rJPV or rJPVΔSH at an MOI of 5. At 2 d.p.i., L929 cells were washed twice with PBS without Mg^{2+} or Ca^{2+} and incubated in 0.5 ml of TTE buffer (0.2% Triton X-100, 10 mM Tris, 15 mM EDTA, pH 8.0) at room temperature for 15 min. Cell lysates were harvested and centrifuged at 14,000 rpm for 20 min. Supernatants were digested with 100 μg of RNase A/ml at 37°C for 1 h. Samples were purified by phenol-chloroform extraction, precipitated, and washed with 70% ethanol. Pellets were air dried and resuspended in 10 μl of Tris-EDTA. Electrophoresis was performed on 2% agarose gels with size markers.

For terminal deoxynucleotidyltransferase-mediated dUTP-biotin nick end labeling (TUNEL) assay, L929 cells were trypsinized and combined with floating cells in the medium at different time points. The harvested cells were centrifuged and washed with PBS. The cells were fixed and permeabilized. The cells were then incubated with 25 μl of TUNEL reaction mixture (cell death detection kit; Roche Diagnostics Corp., Mannheim, Germany) for 2 to 3 h in the dark at 37°C. The cells were analyzed by flow cytometry (Invitrogen Corporation, Carlsbad, CA).

Antibody treatment of infected cells. Confluent L929 cells were mock infected or infected with rJPV or rJPVΔSH at an MOI of 5 and were incubated in 0.5 ml of DMEM–2% FBS with neutralizing antibody against TNF-α (BD Pharmingen, San Jose, CA) or isotype control at 50 μg/ml. At 2 d.p.i., the cells were photographed using a light microscope. The cells were collected, and TUNEL assays were carried out as described above.

Infection of mice with JPV. All animal experiments were carried out strictly following the protocol approved by the IACUC. To study the pathogenesis of JPV in mice, 6-week-old wild-type BALB/cJ mice (Jackson Laboratories) were infected with 50 μl of PBS or 10^5 PFU of rJPV or rJPVΔSH intranasally. The weight of the mice was monitored daily up to 7 days postinfection. Mice were euthanized at 1, 3, and 7 days postinfection to collect sera and tissues, including lungs. To preserve the morphology for histology studies, lungs were inflated with 4% paraformaldehyde. Tissues were fixed in 4% paraformaldehyde at 4°C.

Histology studies. BALB/cJ mice from the infection study were euthanized by asphyxiation. The lungs were inflated with 4% paraformaldehyde and collected. Samples were routinely processed, embedded, and sectioned for hematoxylin-and-eosin (H&E) staining. Alveolar infiltrates and perivascular cuffing were scored from 1 (minimal) to 4 (severe) in a blinded fashion by a board-certified veterinary pathologist. Photomicrographs were taken using an Olympus BX41 microscope with an Olympus DP70 microscope digital camera and DP Controller imaging software.

RESULTS

Rescue of recombinant JPV. The plasmids containing the individual genes for N, P, M, F, SH, TM, G, and L were used to construct a full-length cDNA of the JPV genome in a plasmid (pJPV). Synthetic oligonucleotide linkers spanning the intercistronic junction, leader, and trailer sequences were used to join together these individual genes by PCR. The plasmid containing the JPV cDNA was flanked by a T7 RNA polymerase (RNAP) promoter and a hepatitis delta virus ribozyme followed by a T7 terminator (T7-T) (Fig. 1A). pJPV, carrying the full-length genome of JPV, and three helper plasmids, pJPV-N, pJPV-P, and pJPV-L, carrying the N, P, and L proteins, respectively, were cotransfected into BSR-T7 cells. After obtaining the rescued virus, RT-PCR was used to confirm the recombinant virus with primers specific for the JPV sequence (data not shown). A unique NotI site was introduced into the 3′ noncoding region of ORF-X by replacing four nucleotides to facilitate DNA cloning and as a sequence marker. The recovery was further confirmed by using RT-PCR to amplify the region containing the NotI site. After NotI digestion, two small fragments of 611 and 233 bp were obtained. Nucleotide sequencing of the purified PCR product confirmed the introduced NotI sequence tag (Fig. 1B). The full-length genome sequence of rJPV was determined using 22 pairs of primers for PCRs and 44 primers for sequencing. One plaque-purified clone of rJPV containing the exact viral genome sequence of the cDNA was used for further experiments. To further confirm the recombinant virus, we examined the expression of the TM protein, a unique JPV protein, in rJPV-infected Vero cells using immunofluorescent staining (Fig. 1C). The TM protein was only detected in rJPV-infected cells and not in mock-infected cells, indicating rescue of infectious JPV.

We inserted an extra gene, enhanced green fluorescent protein (EGFP), with the gene end (GE) of the F gene and gene start (GS) of the SH gene between the F and SH genes of the JPV genome. The viral genome length was engineered to conform to the rule of six. The full-length genome sequence of rJPV-EGFP was determined using 23 pairs of primers for PCRs and 46 primers for sequencing. One plaque-purified clone of rJPV-EGFP containing the exact viral genome sequence of the cDNA was used for further experiments. To confirm the rescue of rJPV-EGFP virus, Vero cells were infected with rJPV or rJPV-EGFP and examined using a fluorescence microscope (Fig. 1D). rJPV-EGFP-infected Vero cells showed a strong fluorescence signal, whereas rJPV-infected cells showed no signal, indicating expression of EGFP. The virus was further confirmed using RT-PCR (data not shown).

To construct a plasmid lacking the SH gene, we replaced the ORF of the SH gene with the ORF of the *Renilla* luciferase (Rluc) gene (Fig. 2A). The viral genome length was engineered to conform to the rule of six. RT-PCR amplifying the region between the F and TM genes was used to confirm the rescue. The ORF of Rluc was about 726 bp longer than that of the SH gene, and there were different GE/GS sequences in two constructs, so the amplified fragment was about 878 bp in rJPV-infected cells or 1,568 bp in rJPVΔSH-infected cells (Fig. 2B). The full-length genome sequence of rJPVΔSH was determined using 25 pairs of primers for PCRs and 50 primers for sequencing. One plaque-purified clone of rJPVΔSH containing the exact viral

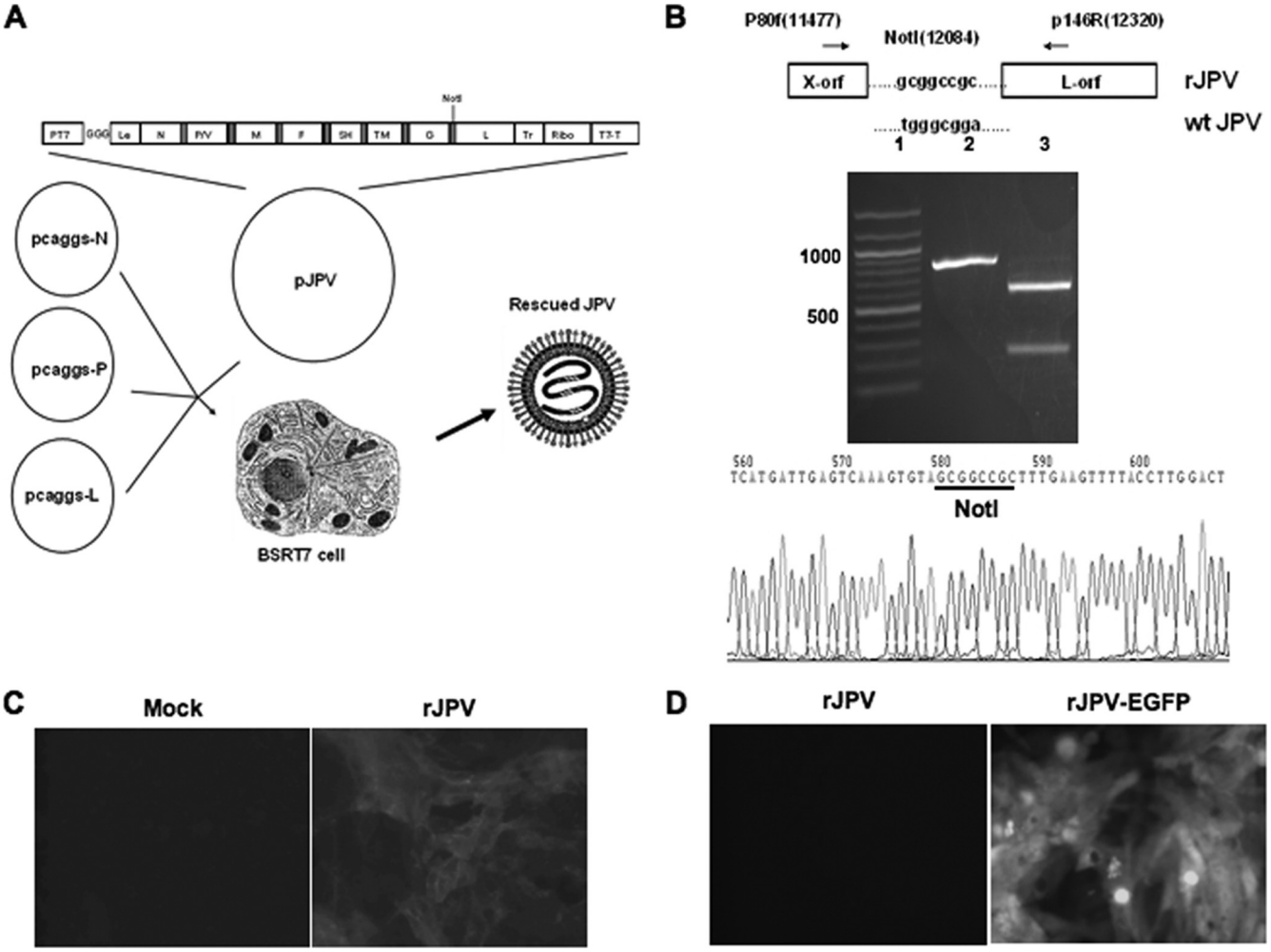

FIG. 1. Recovery of rJPV and rJPV-EGFP. (A) Schematic diagram of the rescue of infectious JPV from its cDNA clone. pJPV contains a complete copy of the JPV genome (18,954 nucleotides) that was flanked by a bacteriophage T7 RNA polymerase (RNAP) promoter (PT7) and a hepatitis delta virus ribozyme followed by a bacteriophage T7 RNAP transcriptional terminator (T7-T). T7 RNA transcripts can be synthesized under the control of the T7 promoter to yield antisense (+) JPV RNA. pJPV contains three extra G residues after the T7 RNAP promoter and prior to the JPV leader (Le) sequence to increase T7 RNAP transcription initiation efficiency. A full-length anti-genome sense JPV RNA transcript can be transcribed from the T7 RNAP promoter with the exact trailer sequence generated by cleavage with hepatitis delta virus ribozyme. The filled boxes indicate the seven intercistronic regions. A sequence tag (NotI site) is introduced into the 3′ noncoding region of ORF-X. Plasmids pCAGGS-N, pCAGGS-P, and pCAGGS-L contain the cDNA for the JPV N, P, and L proteins, respectively. BSR-T7 cells were cotransfected with pJPV and the three plasmids pCAGGS-N, pCAGGS-P, and pCAGGS-L. The transfection medium was replaced with DMEM containing 10% FBS and 10% TPB after 3 h of incubation, and the cultures were incubated for 72 h. The BSR-T7 cells were passaged with Vero cells and cocultured for 2 weeks. Tr, trailer sequence of JPV; Ribo, ribozyme from hepatitis delta virus. (B) Detection of the new NotI site. Top: schematic diagram of NotI site introduced into the 3′ noncoding region of ORF-X. The NotI site was introduced into the 3′ noncoding region of ORF-X by PCR mutagenesis. P90f and p46R are the primers used for RT-PCR; the locations of the primers are shown in parentheses. wt, wild type. Middle: RT-PCR results for RNA from rJPV-infected Vero cells. Lane 1, DNA size marker with relevant sizes indicated. Lane 2, RNA from virus-infected cells using primers p80 and p146; the expected size of the PCR product was 844 bp. Lane 3, PCR product from lane 2 cut with NotI. The two bands were 611 and 233 bp in size. Bottom: sequencing result for PCR product. The NotI recognition sequence, GCGGCCGC, is underlined. (C) Immunofluorescent staining patterns of rJPV-infected cells. Vero cells were mock infected or infected with rJPV. At 2 d.p.i., cells were fixed with 1% formaldehyde and permeabilized with 0.1% saponin. Cells were stained with polyclonal antibody against TM rabbit sera and FITC-conjugated goat anti-rabbit secondary antibody. Fluorescence was examined using a Nikon FXA fluorescence microscope. (D) EGFP expression of rJPV-EGFP virus. Vero cells were infected with rJPV or rJPV-EGFP. At 48 h p.i., fluorescence was examined using a Nikon FXA fluorescence microscope.

genome sequence of the cDNA was used for the subsequent experiments. To confirm the mutant virus lacking the expression of SH, an immunofluorescence assay was used. Vero cells were mock infected or infected with rJPV or rJPVΔSH. SH protein was only detected in rJPV-infected cells and not in mock- or rJPVΔSH-infected Vero cells (Fig. 2C). *Renilla* luciferase activity was examined, and little luciferase activity was detected in mock- or rJPV-infected Vero cells; however, high luciferase activity was detected in rJPVΔSH-infected Vero cells (Fig. 2D).

Growth kinetics. We examined the growth rates of rJPV and rJPVΔSH in Vero cells at MOIs of 5 and 0.1, respec-

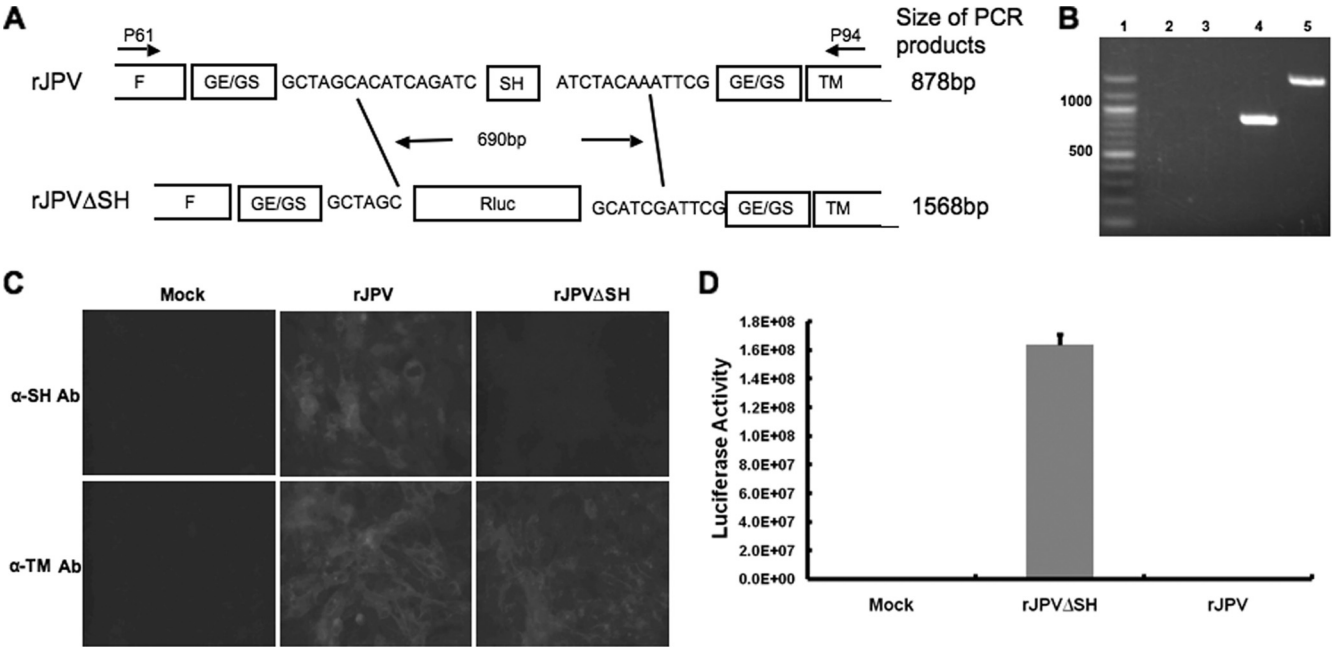

FIG. 2. Recovery of rJPVΔSH. (A) Structure of the rJPV and rJPVΔSH genomes. The SH ORF was replaced with the *Renilla* luciferase gene ORF. (B) RT-PCR results for RNA from rJPV- or rJPVΔSH-infected Vero cells. Lane 1, DNA size marker with relevant sizes indicated. Lanes 2 and 3, RNA from virus-infected cells with reverse transcriptase omitted from RT-PCR. Lanes 4 and 5, RNA from virus-infected cells. In lanes 4 and 5, the sizes of the PCR products were 878 bp for rJPV and 1,568 bp for rJPVΔSH using primers p61 (within the F gene) and p94 (within the TM gene). (C) Immunofluorescent staining patterns of rJPV- and rJPVΔSH-infected cells. Vero cells were mock infected or infected with rJPV or rJPVΔSH. At 2 d.p.i., the cells were fixed with 0.5% formaldehyde and permeabilized with 0.1% saponin. Cells were stained with rabbit polyclonal antibody (Ab) against SH or TM and with FITC-conjugated goat anti-rabbit secondary antibody. Fluorescence was examined using a Nikon FXA fluorescence microscope. (D) Rluc activity assay. Vero cells in 24-well plates were mock infected or infected with rJPV or rJPVΔSH. At 1 d.p.i., cells were lysed to examine Rluc activity using a luminometer according to the manufacturer's instructions. Error bars show standard errors of the means.

tively. The medium was harvested at different time points to determine virus titers by plaque assay. No difference in the plaque sizes of rJPV and rJPVΔSH was observed (data not shown). rJPV and rJPVΔSH showed similar growth rates in single-step (Fig. 3A) and multiple-step (Fig. 3B) growth curves.

We examined the levels of expression of P and V proteins by rJPV and rJPVΔSH by using specific rabbit polyclonal serum against P or V protein. No difference was observed by immunoprecipitation assay (Fig. 3C).

rJPVΔSH induced apoptosis in L929 cells. Paramyxoviruses lacking SH induce apoptosis in L929 cells through a TNF-α-mediated pathway. To investigate the phenotypes of rJPV and rJPVΔSH in L929 cells, cells were mock infected or infected with rJPV or rJPVΔSH at an MOI of 5. CPE was observed in rJPV- or rJPVΔSH-infected L929 cells (Fig. 4A). rJPV and rJPVΔSH both induced CPE, and there were more dead cells in rJPVΔSH-infected cells.

To investigate whether the CPE induced by rJPV or rJPVΔSH was due to apoptosis and whether there was a difference in the extent of apoptosis induced by rJPV or rJPVΔSH, we examined the fragmented DNA in rJPV- and rJPVΔSH-infected L929 cells. Cells were mock infected or infected with rJPV or rJPVΔSH at an MOI of 5. At 2 d.p.i., cells were collected and DNAs were extracted and resolved in 2% agarose gel. Fragmented DNA was not detected in the mock-infected cells; however, small amounts of fragmented DNA were found in the rJPV-infected cells, and increasing amounts of fragmented DNA were detected in rJPVΔSH-infected cells (Fig. 4B), suggesting that rJPV and rJPVΔSH induced apoptosis in cells but rJPVΔSH caused greater apoptosis.

To quantify the apoptosis induced by rJPV or rJPVΔSH, a TUNEL assay was used. At 1 d.p.i. and 2 d.p.i., cells were collected for TUNEL assay. At 1 d.p.i., about 1.3% of cells infected by rJPV were apoptotic, compared to 2.9% of cells infected by rJPVΔSH. At 2 d.p.i., approximately 20% of cells infected by rJPV were apoptotic, compared to 38% of cells infected by rJPVΔSH (Fig. 4C). These data suggest that while rJPV induced cell apoptosis at a basal level, rJPVΔSH induced greater apoptosis.

To investigate the mechanism of rJPVΔSH-induced apoptosis, the ability of culture medium from the infected cells to cause CPE was examined. L929 cells were infected with rJPV or rJPVΔSH at an MOI of 5 for 2 days. The culture medium from the infected cells was collected, UV irradiated to inactivate viruses, and filtered through 0.22-μm filters to remove cell debris. Complete inactivation of virus by UV irradiation was confirmed by plaque assay (data not shown). The medium was then added to fresh L929 cells. After 2 days of incubation, CPE was observed in the cells incubated with UV-treated medium from rJPV- and rJPVΔSH-infected cells (Fig. 4D). However, the CPE was greater in the cells incubated with UV-treated medium from rJPVΔSH-

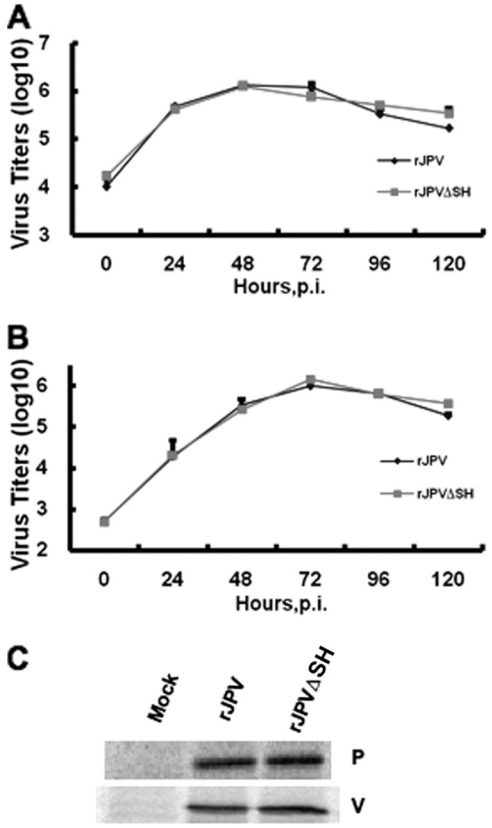

FIG. 3. Comparison of rJPV and rJPVΔSH *in vitro*. (A) Single-step growth curves of rJPV and rJPVΔSH. Vero cells were infected with rJPV or rJPVΔSH at an MOI of 5, and the medium was harvested at 24-h intervals. The titers of the viruses were determined by plaque assay on Vero cells. (B) Multiple-step growth curves of rJPV and rJPVΔSH. Vero cells were infected with rJPV or rJPVΔSH at an MOI of 0.1, and the medium was harvested at 24-h intervals. The titers of the viruses were determined by plaque assay on Vero cells. (C) Analysis of P protein and V protein synthesized by rJPV and rJPVΔSH. Vero cells were mock infected or infected with rJPV or rJPVΔSH. At 22 h p.i., the cells were labeled with ^{35}S-Met/Cys Promix for 2 h and then lysed in radioimmunoprecipitation buffer and immunoprecipitated using polyclonal antibody against P protein or V protein.

infected cells than in those incubated with UV-treated medium from rJPV-infected cells. Very little CPE was observed in cells incubated in UV-treated medium from mock infection. This result shows that components secreted from virus-infected cells can cause CPE in L929 cells, suggesting that proteins, such as cytokines induced by virus infection, may be involved in apoptosis induced by viral infection. The difference in the severity of the CPE caused by incubation with the UV-treated medium from rJPV- or RJPVΔSH-infected cells suggests that more of the apoptosis-inducing protein was produced by rJPVΔSH-infected cells.

Previous studies showed that there was a higher level of production of TNF-α by rPIV5ΔSH-infected L929 cells than wild-type rPIV5-infected L929 cells. To investigate the involvement of TNF-α in rJPV- and rJPVΔSH-induced CPE in L929 cells, the production of TNF-α by infected cells was measured by ELISA. Increased levels of TNF-α were detected, and the level of TNF-α in rJPVΔSH-infected cells was higher than that in rJPV-infected cells (Fig. 4E).

Inhibition of rJPVΔSH-induced apoptosis by neutralizing antibody against TNF-α. To study whether TNF-α was responsible for apoptosis induction in rJPV- and rJPVΔSH-infected cells, L929 cells were infected with rJPV or rJPVΔSH at an MOI of 5 and were incubated with no antibody, isotype control antibody, or neutralizing antibody against TNF-α at 50 μg/ml. The CPE caused by rJPV and rJPVΔSH was inhibited by the neutralizing antibody, while no inhibition was observed in the cells incubated with control antibody (Fig. 5A). The ability of TNF-α neutralizing antibody to inhibit apoptosis was quantified by TUNEL assay using flow cytometry. As shown by the results in Fig. 5B, apoptosis induced by rJPVΔSH infection was inhibited when the infected cells were incubated with the neutralizing antibody against TNF-α but not when the cells were incubated with control antibody. Anti-TNF-α antibody also reduced apoptosis induced by rJPV.

Activation of NF-κB and inhibition of TNF-α-induced NF-κB activation. TNF-α can activate NF-κB, and the activated NF-κB can further upregulate the expression of TNF-α. To examine the activation of NF-κB by rJPVΔSH, L929 cells were mock infected or infected with rJPV or rJPVΔSH, and then immunofluorescence staining for p65 was performed. The numbers of positive cells from 10 randomly chosen fields per group were calculated. As shown by the results in Fig. 6A, mock-infected cells showed no nuclear translocation of p65, a key subunit of NF-κB. Twenty-nine percent of the rJPV-infected cells showed nuclear p65, compared to 50% of rJPVΔSH-infected cells. This suggests that rJPV activated NF-κB and rJPVΔSH induced greater p65 translocation into the nucleus, indicating that the SH protein may play a role in blocking NF-κB activation. To investigate whether JPV SH protein can inhibit TNF-α-induced NF-κB activation, a plasmid with the firefly luciferase gene under the control of an NF-κB TATA promoter was used as a reporter gene. The reporter gene construct, along with a transfection control plasmid, phRL-TK, which has *Renilla* luciferase under the control of a herpes simplex virus TK promoter, were transfected with either an empty vector or a vector containing a gene encoding JPV SH or PIV5 SH. The average increases in luciferase activity (*n*-fold) in cells treated with TNF-α were significantly smaller than the increases in luciferase activity in untreated cells, indicating that JPV SH protein inhibited TNF-α-induced NF-κB activation (Fig. 6B). Interestingly, SH had no effect on the PMA-mediated NF-κB activation, which activates NF-κB through a protein kinase C-dependent pathway (8), suggesting that the step of the inhibition of NF-κB by SH is upstream of NF-κB (Fig. 6C).

Infection of mice with rJPV and rJPVΔSH. Since JPV was originally isolated from rodents, we decided to use the mouse as an infection model for studies of JPV pathogenesis. BALB/c mice were intranasally infected with 50 μl of PBS or 10^5 PFU rJPV or rJPVΔSH. Weights were monitored daily up to 7 days. There were no observed clinical signs of illness or weight loss. The mice were sacrificed and organs such lung, kidney, heart, and liver, as well as serum samples, were collected at 1, 3, and 7 d.p.i. No gross pathological changes were observed in the organs. However, histopathology revealed increased lymphocytic perivascular cuffing in mice infected with rJPVΔSH compared to that in mice infected

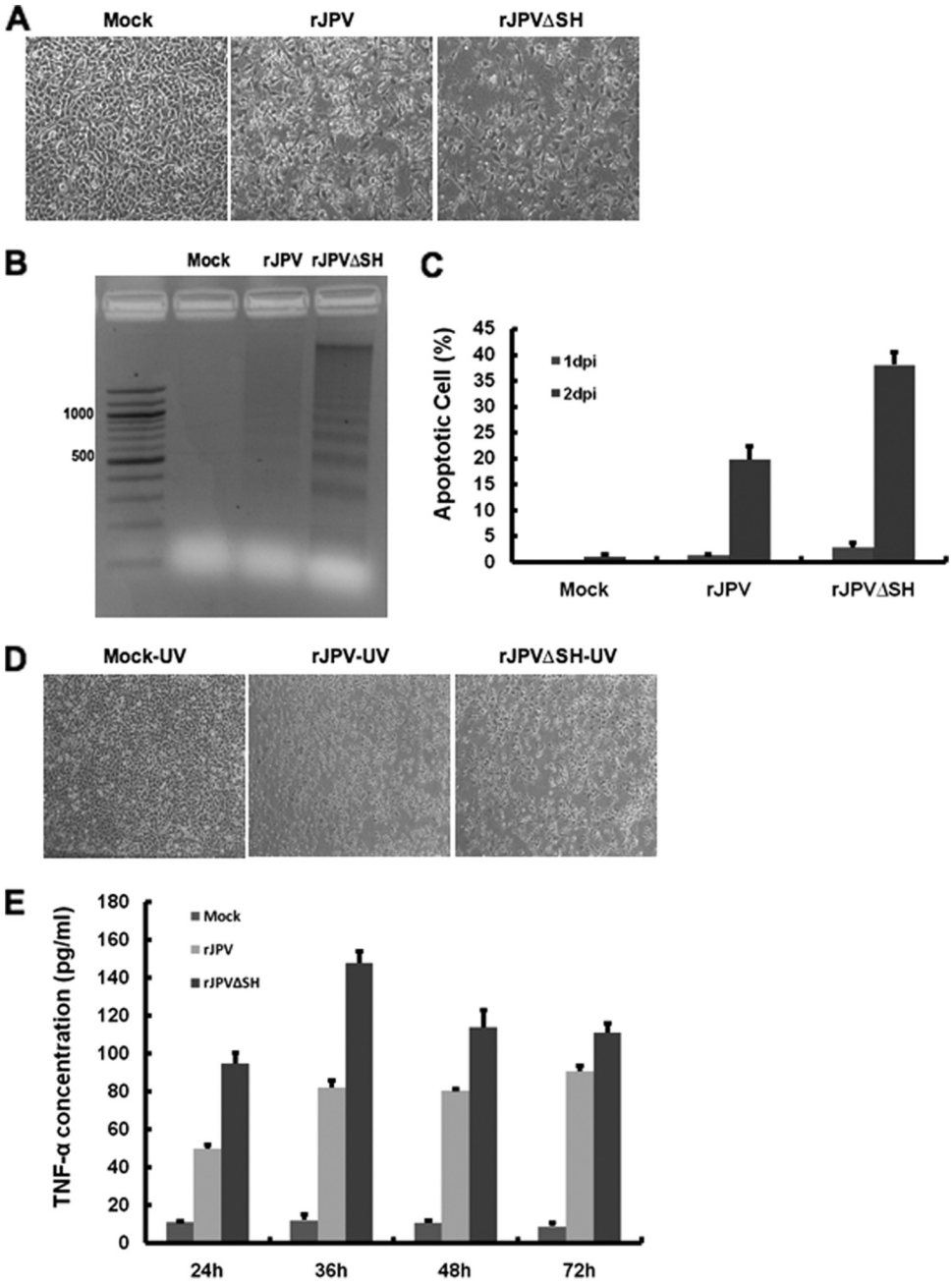

FIG. 4. rJPVΔSH induced apoptosis in L929 cells. (A) CPE induced by rJPV and rJPVΔSH infection in L929 cells. L929 cells were mock infected or infected with rJPV or rJPVΔSH at an MOI of 5. At 2 d.p.i., the cells were photographed. (B) Increased DNA laddering in rJPVΔSH-infected cells. L929 cells were mock infected or infected with rJPV or rJPVΔSH at an MOI of 5. The first lane on the left shows DNA size markers. The cells were collected at 2 d.p.i. (C) Induction of apoptosis by rJPV and rJPVΔSH viruses. L929 cells were mock infected or infected with rJPV or rJPVΔSH at an MOI of 5. The cells were collected for TUNEL assay at the times indicated. (D) L929 cells were infected at an MOI of 5. At 2 d.p.i., the culture medium was UV irradiated and the UV-treated medium was used to replace the regular growth medium for L929 cells. After 2 days of incubation, the cells were photographed. (E) Concentrations of TNF-α produced from rJPV- and rJPVΔSH-infected cells. L929 cells were mock infected or infected with rJPV or rJPVΔSH. The medium was taken at different time points after infection. The amounts of TNF-α were measured by ELISA. Samples are triplicates, and error bars show standard errors of the means.

with rJPV (Fig. 7A). Increased serum levels of TNF-α were detected in rJPVΔSH-infected animals, consistent with the results showing rJPVΔSH induction of a higher level of TNF-α expression in tissue culture cells (Fig. 7B), suggesting that SH plays a role in reducing the expression of TNF-α in infected animals.

DISCUSSION

Members of the subfamily *Paramyxovirinae* contain a conserved genome with the nucleocapsid (N), phosphoprotein (P), matrix (M), fusion (F), attachment (HN/H/G), and

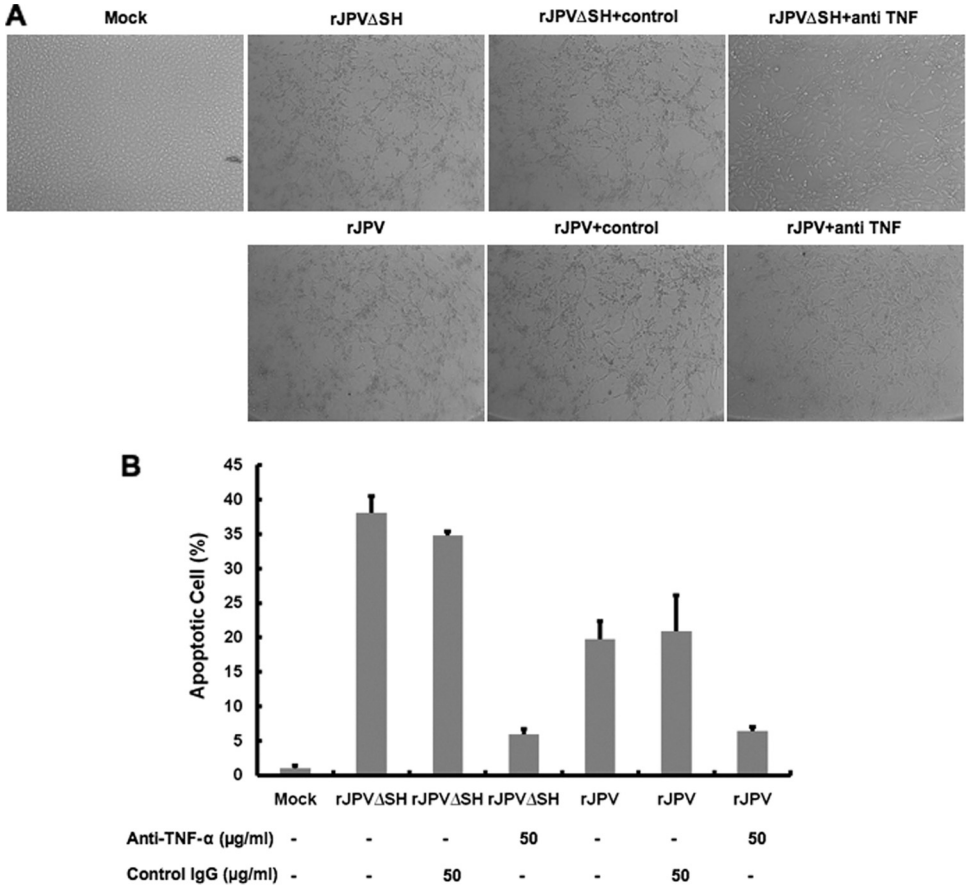

FIG. 5. Anti-TNF-α inhibited rJPV- and rJPVΔSH-induced apoptosis. (A) Inhibition of CPE by the neutralizing antibody against TNF-α. L929 cells were mock infected or infected with rJPV or rJPVΔSH at an MOI of 5 and incubated with no antibody, isotype control antibody (50 μg/ml), or TNF-α neutralizing antibody (50 μg/ml) for 2 days. (B) Inhibition of apoptosis by neutralizing antibody against TNF-α. L929 cells were mock infected or infected with rJPV or rJPVΔSH at an MOI of 5 and incubated with no antibody, control antibody (50 μg/ml), or neutralizing antibody (50 μg/ml) for 2 days. TUNEL assays were carried out at 2 d.p.i. Error bars show standard errors of the means.

large (L) genes found in all viruses (21). Compared to other paramyxoviruses, JPV contains two additional genes, SH and TM with unknown functions. In this work, we studied the function of the SH protein *in vitro* and *in vivo*. Previously, recombinant viruses with SH deleted from PIV5 and RSV have been generated. However, this is the first time an ORF of the SH protein has been replaced with a foreign gene without changing the native GS and GE sequences of the SH gene, avoiding potential issues of deleting an entire transcriptional unit (as in PIV5ΔSH) (10) or creating a chimeric GE/GS (as in RSVΔSH) (9). Furthermore, since JPV was isolated from rodents, using a mouse model resembles the natural infection. At present, it is not clear what the natural host is for PIV5, and the only small animal model available is based on an immunodeficient mouse ($Stat1^{-/-}$) (11, 12). RSV is a human pathogen, and therefore, the mouse is not an ideal model for studies of RSV pathogenesis. Using a mouse model, we have found that the deletion of SH in JPV led to increased expression of TNF-α in infected mice, confirming our *in vitro* work. With a reverse genetics system and a small-animal model, JPV may serve as a good model to study the pathogenesis of paramyxoviruses. For the first time, we have confirmed that the lack of SH results in an increase in TNF-α expression in infected animals. Interestingly, we did not observe severe pathological changes in the lungs of infected animals. This differs from the report indicating that JPV causes hemorrhagic interstitial pneumonia (19). It is possible that the virus we generated, based on a sequence from a virus that is several generations away from the original isolate, has adapted to growth in the laboratory and may contain mutations. BeiPV, an unclassified paramyxovirus, was isolated from rat and human mesangial cell lines in 2006 (22). BeiPV contains 8 identical genes in the same order as JPV. Two additional ORFs, named X1 and X2, in the 3′ untranslated region (UTR) of the G gene have been proposed. X1 is in the +3 reading frame and X2 is in the +2 reading frame, overlapping by 31 nucleotides with X1. The amino acid sequence identity between cognate proteins of JPV and BeiPV ranges from 27 to 80%. The six proteins present in all paramyxoviruses (N, P, M, F, G, and L) display medium to high homology (47 to 80%), whereas the SH and TM proteins have low but significant homology (27 and 35%). It is likely that BeiPV and JPV form a novel genus of the paramyxo-

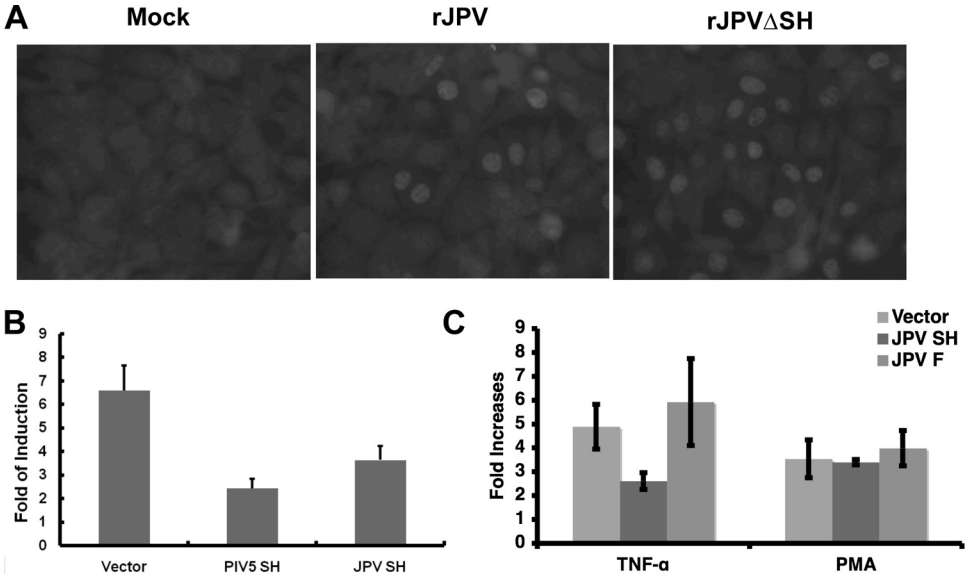

FIG. 6. Activation of NF-κB and inhibition of TNF-α-induced NF-κB activation. (A) Activation of NF-κB. L929 cells were mock infected or infected with rJPV or rJPVΔSH at an MOI of 5. At 1 d.p.i., the cells were fixed with 0.5% formaldehyde and permeabilized with 0.1% saponin. Cells were incubated with rabbit antibody against the mouse p65 subunit of NF-κB and with FITC-conjugated goat anti-rabbit secondary antibody. Fluorescence was examined using a Nikon FXA fluorescence microscope. (B) JPV SH protein inhibits TNF-α-induced NF-κB activation. L929 cells were transfected with pCAGGS, pCAGGS-PIV5 SH, or pCAGGS-JPV SH together with pκB-TATA-luc and phRL-TK. At 1 day posttransfection, the medium was replaced with Opti-MEM or Opti-MEM and TNF-α (10 ng/ml). The cells were incubated for 4 h at 37°C. NF-κB activation was determined using a Veritas microplate luminometer. Luciferase activity was measured as the ratio of firefly luciferase activity to *Renilla* luciferase activity. The fold increase, as determined by the ratio of the amount of luciferase activity of TNF-treated cells to that of untreated cells, is shown. Error bars show standard errors of the means. (C) Effect of SH on PMA-mediated NF-κB activation. The same experiment as described for panel B was performed using Opti-MEM containing PMA (50 ng/ml), as well as TNF-α to stimulate the transfected cells.

virus family. The functions of the viral proteins and pathogenesis of the viruses have not been well studied. Our work in generating a reverse genetics system for JPV will aid future studies of these novel and emerging viruses.

PIV5, MuV, and RSV encode the SH protein, which has been shown to play an essential role in blocking apoptosis in infected cells through inhibition of the TNF-α pathway (9, 23, 31). Since rJPVΔSH-infected cells produced more TNF-α than rJPV-infected cells during infection, this suggests that the JPV SH protein plays an important role in the inhibition of TNF-α production, like the SH proteins of other paramyxoviruses. Results showing that ectopically expressed JPV SH blocked the activation of p65 by TNF-α further confirmed that SH blocks TNF-α signaling. Neutralizing antibody against TNF-α inhibited cell apoptosis induced by rJPVΔSH, as expected. Interestingly, the neutralizing antibody against TNF-α also reduced apoptosis induced by wild-type JPV, suggesting that the JPV SH is not effective in blocking apoptosis mediated by TNF-α. Since TNF-α can induce multiple signaling pathways, one leading to activation of apoptosis and one leading to the activation of NF-κB and TNF-α expression (autocrine) (1), we speculate that JPV SH is most effective at blocking the pathway leading to the activation of NF-κB that triggers TNF-α expression. It is possible that the initial production of TNF-α in the cells infected with JPV is triggered by virus replication (such as viral proteins). NF-κB upregulates the expression of TNF-α. TNF-α is an autocrine cytokine. More TNF-α is produced in infected cells lacking SH (hence the increased expression of TNF-α in rJPVΔSH-infected cells). It is also possible that at lower concentrations, TNF-α-mediated cell death can be blocked by SH. This is consistent with increased TNF-α concentrations and increased apoptosis in JPV-infected cells. Thus, JPV SH may play a role in blocking cell death at a low concentration of TNF-α (at 1 d.p.i. in wild-type JPV-infected cells), thus delaying apoptosis. By timing the apoptosis to a later stage, it may represent an advantage for viral spread while evading host inflammatory responses, as well as avoiding premature death of host cells.

Nonsegmented negative-strand RNA viruses (NNSVs) are potential viral vector candidates for vaccine development. In comparison to DNA viruses, the NNSVs do not have a DNA phase in their life cycles and replicate in the cytoplasm, thus avoiding unintended consequences from genetic modifications of host cell DNA that may be associated with recombination or insertion (21). Compared to those of positive-strand RNA viruses, the genomes of NNSVs are stable. NNSV genomes are relatively simple, more fully understood, and easier to manipulate. These characteristics make NNSVs useful as potential vaccine vectors. PIV5, vesicular stomatitis virus, human PIV3, measles viruses, Sendai viruses, and Newcastle disease virus have been used for vaccine research (24–26, 29, 30). As JPV has one of the largest genomes in the paramyxovirus family, it is conceivable that there is a greater capacity for the JPV genome to express larger foreign genes. To examine whether the JPV genome can be used as a vector to express foreign genes, we

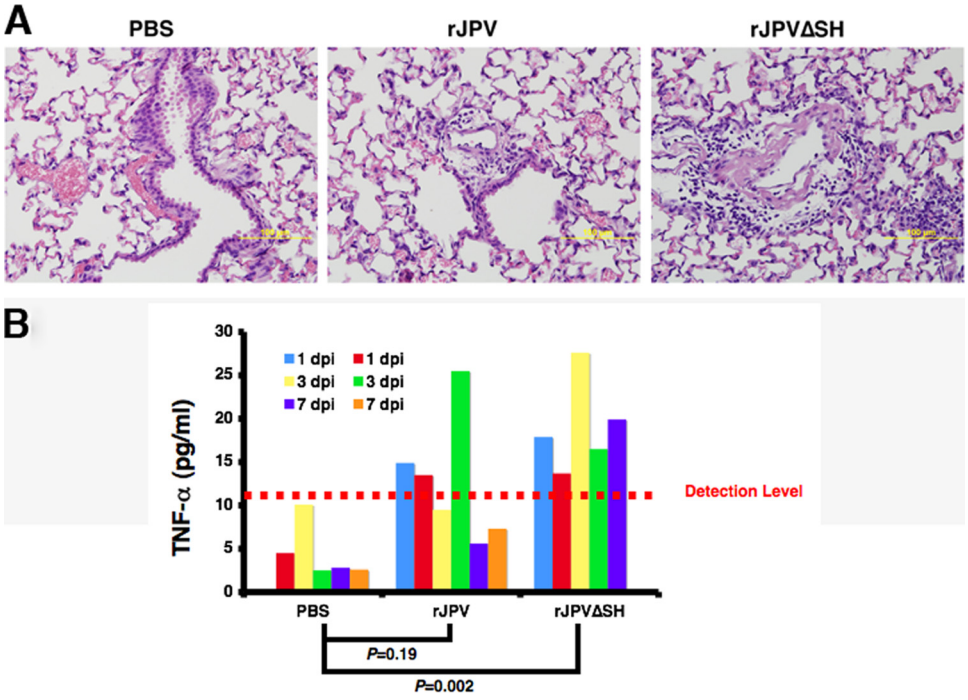

FIG. 7. Infection of animals with rJPV and rJPVΔSH. (A) Histopathology of lungs from infected animals. Lung samples from BALB/c mice infected with PBS or 10^5 PFU rJPV or rJPVΔSH were taken 3 days after intranasal infection. Photomicrographs show representative perivascular lesions for each group. (B) Concentrations of serum TNF-α in infected BALB/c mice. Sera were collected from infected animals ($n = 5$ for PBS and rJPVΔSH, and $n = 6$ for rJPV) at different time points after infection. Levels of TNF-α were measured using ELISA.

inserted the EGFP gene into the JPV genome, demonstrating the feasibility of this approach.

ACKNOWLEDGMENTS

We thank the members of Biao He's laboratory for helpful discussions and technical assistance.

The work was supported by grants from the National Institute of Allergy and Infectious Diseases and Georgia Research Alliance to B.H. (grant numbers AI070847 and K02 AI65795).

REFERENCES

1. **Baud, V., and M. Karin.** 2001. Signal transduction by tumor necrosis factor and its relatives. Trends Cell Biol. **11:**372–377.
2. **Buchholz, U. J., S. Finke, and K. K. Conzelmann.** 1999. Generation of bovine respiratory syncytial virus (BRSV) from cDNA: BRSV NS2 is not essential for virus replication in tissue culture, and the human RSV leader region acts as a functional BRSV genome promoter. J. Virol. **73:**251–259.
3. **Bukreyev, A., S. S. Whitehead, B. R. Murphy, and P. L. Collins.** 1997. Recombinant respiratory syncytial virus from which the entire SH gene has been deleted grows efficiently in cell culture and exhibits site-specific attenuation in the respiratory tract of the mouse. J. Virol. **71:**8973–8982.
4. **Chatziandreou, N., N. Stock, D. Young, J. Andrejeva, K. Hagmaier, D. J. McGeoch, and R. E. Randall.** 2004. Relationships and host range of human, canine, simian and porcine isolates of simian virus 5 (parainfluenza virus 5). J. Gen. Virol. **85:**3007–3016.
5. **Collins, P. L., R. A. Olmsted, and P. R. Johnson.** 1990. The small hydrophobic protein of human respiratory syncytial virus: comparison between antigenic subgroups A and B. J. Gen. Virol. **71**(Pt. 7)**:**1571–1576.
6. **Collins, P. L., and G. W. Wertz.** 1985. The 1A protein gene of human respiratory syncytial virus: nucleotide sequence of the mRNA and a related polycistronic transcript. Virology **141:**283–291.
7. **Elango, N., J. Kovamees, T. M. Varsanyi, and E. Norrby.** 1989. mRNA sequence and deduced amino acid sequence of the mumps virus small hydrophobic protein gene. J. Virol. **63:**1413–1415.
8. **Feuillard, J., H. Gouy, G. Bismuth, L. M. Lee, P. Debre, and M. Korner.** 1991. NF-kappa B activation by tumor necrosis factor alpha in the Jurkat T cell line is independent of protein kinase A, protein kinase C, and Ca(2+)-regulated kinases. Cytokine **3:**257–265.
9. **Fuentes, S., K. C. Tran, P. Luthra, M. N. Teng, and B. He.** 2007. Function of the respiratory syncytial virus small hydrophobic protein. J. Virol. **81:** 8361–8366.
10. **He, B., G. P. Leser, R. G. Paterson, and R. A. Lamb.** 1998. The paramyxovirus SV5 small hydrophobic (SH) protein is not essential for virus growth in tissue culture cells. Virology **250:**30–40.
11. **He, B., G. Y. Lin, J. E. Durbin, R. K. Durbin, and R. A. Lamb.** 2001. The SH integral membrane protein of the paramyxovirus simian virus 5 is required to block apoptosis in MDBK cells. J. Virol. **75:**4068–4079.
12. **He, B., R. G. Paterson, N. Stock, J. E. Durbin, R. K. Durbin, S. Goodbourn, R. E. Randall, and R. A. Lamb.** 2002. Recovery of paramyxovirus simian virus 5 with a V protein lacking the conserved cysteine-rich domain: the multifunctional V protein blocks both interferon-beta induction and interferon signaling. Virology **303:**15–32.
13. **He, B., R. G. Paterson, C. D. Ward, and R. A. Lamb.** 1997. Recovery of infectious SV5 from cloned DNA and expression of a foreign gene. Virology **237:**249–260.
14. **Hiebert, S. W., R. G. Paterson, and R. A. Lamb.** 1985. Identification and predicted sequence of a previously unrecognized small hydrophobic protein, SH, of the paramyxovirus simian virus 5. J. Virol. **55:**744–751.
15. **Hiebert, S. W., C. D. Richardson, and R. A. Lamb.** 1988. Cell surface expression and orientation in membranes of the 44-amino-acid SH protein of simian virus 5. J. Virol. **62:**2347–2357.
16. **Jack, P. J., D. E. Anderson, K. N. Bossart, G. A. Marsh, M. Yu, and L. F. Wang.** 2008. Expression of novel genes encoded by the paramyxovirus J virus. J. Gen. Virol. **89:**1434–1441.
17. **Jack, P. J., D. B. Boyle, B. T. Eaton, and L. F. Wang.** 2005. The complete genome sequence of J virus reveals a unique genome structure in the family Paramyxoviridae. J. Virol. **79:**10690–10700.
18. **Jin, H., H. Zhou, X. Cheng, R. Tang, M. Munoz, and N. Nguyen.** 2000. Recombinant respiratory syncytial viruses with deletions in the NS1, NS2, SH, and M2-2 genes are attenuated in vitro and in vivo. Virology **273:**210–218.
19. **Jun, M. H., N. Karabatsos, and R. H. Johnson.** 1977. A new mouse paramyxovirus (J virus). Aust. J. Exp. Biol. Med. Sci. **55:**645–647.
20. **Karron, R. A., D. A. Buonagurio, A. F. Georgiu, S. S. Whitehead, J. E. Adamus, M. L. Clements-Mann, D. O. Harris, V. B. Randolph, S. A. Udem, B. R. Murphy, and M. S. Sidhu.** 1997. Respiratory syncytial virus (RSV) SH and G proteins are not essential for viral replication in vitro: clinical evaluation and molecular characterization of a cold-passaged, attenuated RSV subgroup B mutant. Proc. Natl. Acad. Sci. U. S. A. **94:**13961–13966.
21. **Lamb, R. A., and D. Kolakofsky.** 2001. *Paramyxoviridae*: the viruses and their

replication. *In* D. M. Knipe and P. M. Howley (ed.), Fields virology, 4th ed. Lippincott, Williams and Wilkins, Philadelphia, PA.

22. **Li, Z., M. Yu, H. Zhang, D. E. Magoffin, P. J. Jack, A. Hyatt, H. Y. Wang, and L. F. Wang.** 2006. Beilong virus, a novel paramyxovirus with the largest genome of non-segmented negative-stranded RNA viruses. Virology **346:** 219–228.
23. **Lin, Y., A. C. Bright, T. A. Rothermel, and B. He.** 2003. Induction of apoptosis by paramyxovirus simian virus 5 lacking a small hydrophobic gene. J. Virol. **77:**3371–3383.
24. **Nakaya, T., J. Cros, M. S. Park, Y. Nakaya, H. Zheng, A. Sagrera, E. Villar, A. Garcia-Sastre, and P. Palese.** 2001. Recombinant Newcastle disease virus as a vaccine vector. J. Virol. **75:**11868–11873.
25. **Roberts, A., E. Kretzschmar, A. S. Perkins, J. Forman, R. Price, L. Buonocore, Y. Kawaoka, and J. K. Rose.** 1998. Vaccination with a recombinant vesicular stomatitis virus expressing an influenza virus hemagglutinin provides complete protection from influenza virus challenge. J. Virol. **72:**4704–4711.
26. **Singh, M., R. Cattaneo, and M. A. Billeter.** 1999. A recombinant measles virus expressing hepatitis B virus surface antigen induces humoral immune responses in genetically modified mice. J. Virol. **73:**4823–4828.
27. **Takeuchi, K., K. Tanabayashi, M. Hishiyama, and A. Yamada.** 1996. The mumps virus SH protein is a membrane protein and not essential for virus growth. Virology **225:**156–162.
28. **Takeuchi, K., K. Tanabayashi, M. Hishiyama, A. Yamada, and A. Sugiura.** 1991. Variation of nucleotide sequences and transcription of the SH gene among mumps virus strains. Virology **181:**364–366.
29. **Takimoto, T., J. L. Hurwitz, C. Coleclough, C. Prouser, S. Krishnamurthy, X. Zhan, K. Boyd, R. A. Scroggs, B. Brown, Y. Nagai, A. Portner, and K. S. Slobod.** 2004. Recombinant Sendai virus expressing the G glycoprotein of respiratory syncytial virus (RSV) elicits immune protection against RSV. J. Virol. **78:**6043–6047.
30. **Tompkins, S. M., Y. Lin, G. P. Leser, K. A. Kramer, D. L. Haas, E. W. Howerth, J. Xu, M. J. Kennett, R. K. Durbin, J. E. Durbin, R. Tripp, R. A. Lamb, and B. He.** 2007. Recombinant parainfluenza virus 5 (PIV5) expressing the influenza A virus hemagglutinin provides immunity in mice to influenza A virus challenge. Virology **362:**139–150.
31. **Wilson, R. L., S. M. Fuentes, P. Wang, E. C. Taddeo, A. Klatt, A. J. Henderson, and B. He.** 2006. Function of small hydrophobic proteins of paramyxovirus. J. Virol. **80:**1700–1709.